Microchimica Acta (2021) 188: 205
https://doi.org/10.1007/s00604-021-04854-6

ORIGINAL PAPER

Electrochemiluminescence from a biocatalysis accelerated N-(aminobutyl)-N-(ethylisoluminol)/dissolved O_2 system for microRNA detection

Ying Zhou[1] · Hongxia Liao[1] · Yaqin Chai[1] · Ruo Yuan[1]

Received: 5 January 2021 / Accepted: 11 May 2021 / Published online: 27 May 2021

Abstract

A kind of biocatalyst, laccase, has been employed as a biocompatible coreactant accelerator to efficiently catalyze coreactant (dissolved O_2) for generating high local concentration of superoxide radical ($O_2^{\bullet-}$), acquiring high-intense electrochemiluminescence (ECL) emission of ABEI (N-(aminobutyl)-N-(ethylisoluminol))/dissolved O_2 system. Furthermore, a modified strand displacement reaction with excellent amplification efficiency was constructed by replacing traditional single strand DNA to the hairpin DNA as template for triggering the immobilization of more signal probes. As a result, the biosensor for microRNA-21 determination has preeminent selectivity and favorable sensitivity with detection limit down to 80.8 aM. Significantly, the devised strategy has blazed a new path for seeking more coreaction accelerators with splendid biocompatibility thus promoting the application of ternary ECL systems in biological analysis and clinical diagnosis.

Keywords Laccase · Biocatalysis · Electrochemiluminescence · Biocoreaction accelerator

Introduction

Electrochemiluminescence (ECL), as a promising analytical technique in the biosensing field, has been widely recognized and commended due to low background, wide dynamic range, and ease of control [1, 2]. However, the short lifetime in annihilation reaction lead to weak ECL response of individual electrochemiluminophore for strictly restricting their further application. For many decades, the classical coreactants with strong oxidative, such as H_2O_2, tripropylamine (TPrA), and $S_2O_8^{2-}$, are employed to enhance the luminous efficiency of electrochemiluminophores [3–5]. Among them, dissolved O_2 as an endogenous coreactant possesses great advantages of mild reaction and easy operation which has been researched on facilitating the ECL intensity of luminol and its derivatives, perylene derivative, metal nanoclusters, etc. [6, 7]. But usually, dissolved oxygen is difficultly decomposed into reactive oxide species (ROS) in the surface of electrode, thus generated ROS is too low to offer effective signal amplification. Since the concept of coreaction accelerator has been put forward, various nanomaterials were tried as an alternative to promote the ECL emission of luminol/dissolved O_2 system, containing metals [8], metal oxides [9], and heterojunction nanomaterials [10], et al. Herein, the laccase was first introduced as a biocompatible coreactant accelerator to efficiently bio-catalyze dissolved O_2 for accelerating the generation efficiency of superoxide radical ($O_2^{\bullet-}$), promoting ECL emission of the N-(aminobutyl)-N-(ethylisoluminol) (ABEI)/dissolved O_2 system, in which ABEI as a derivative of luminol, has a primary amine with higher activity than luminol because the amino group is far away from benzene ring.

Here, the template strand of SDA was skillfully designed as a hairpin structure, so that the output strand could not hybridize with the template strand, greatly improving the amplification efficiency and detection specificity. Inspired by these, an ingenious ECL biosensor was fabricated for sensitive determination of target microRNA-21 (miR-21) based on the laccase as biocompatible coreaction accelerator and the improved SDA as a signal amplifier. As shown in Scheme 1, a trace content of miR-21 firstly opened the hairpin template to trigger DNA polymerization based on the template as substrate

✉ Ruo Yuan
yuanruo@swu.edu.cn

[1] Key Laboratory of Luminescent and Real-Time Analytical Chemistry (Southwest University), Ministry of Education, College of Chemistry and Chemical Engineering, Southwest University, Chongqing 400715, China

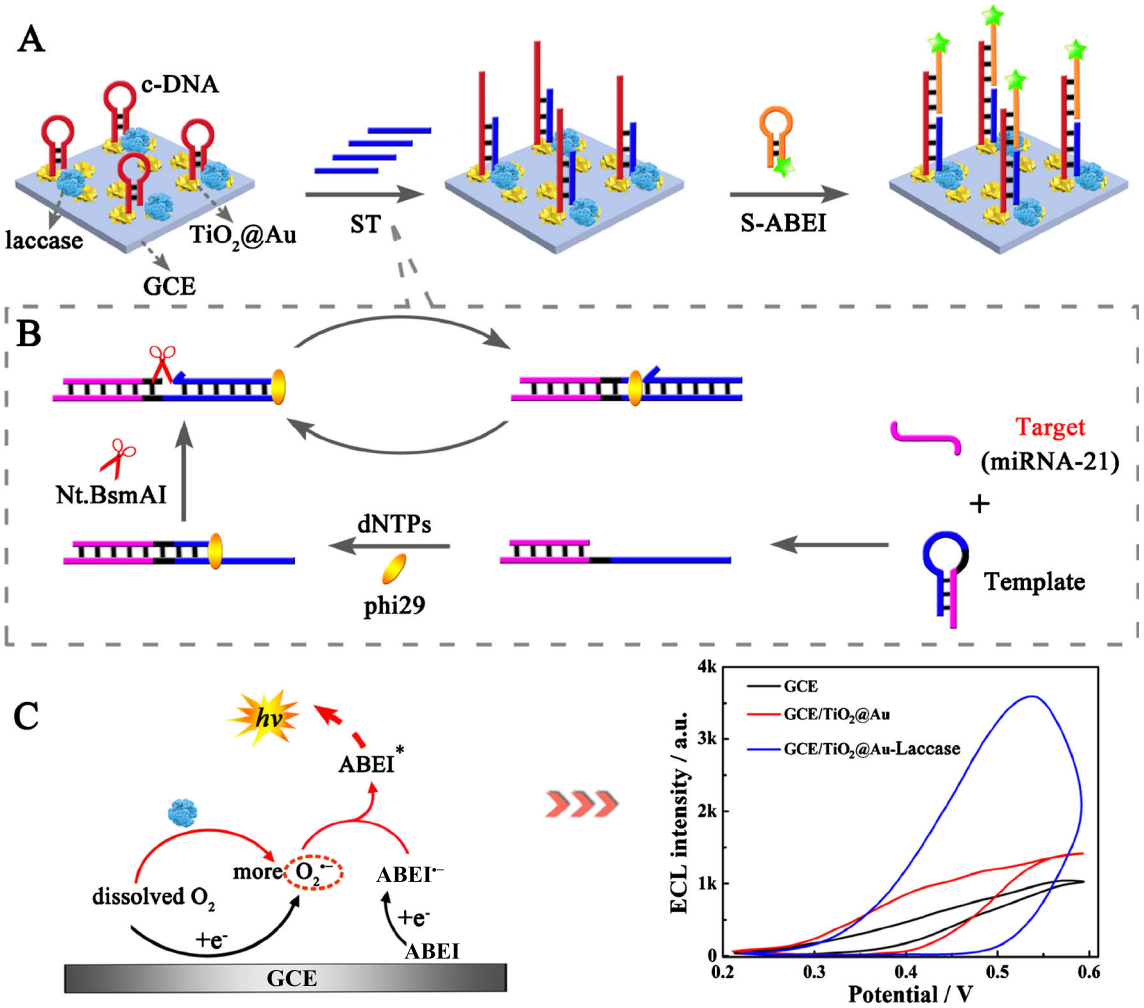

Scheme 1 Schematic diagrams showing (**A**) the target induced meliorative SDA reaction. (**B**) The assembly process of biosensor for miR-21 detection. And (**C**) the mechanism schematic of the ECL system with the promotion of laccase

with the aid of deoxyribonucleoside triphosphates (dNTPs) and phi29 DNA polymerase. Once the splice site of the Nt.BsmAI restriction endonuclease occurred, Nt.BsmAI would cleave the polymerized DNA, and then polymerization reaction proceeded from the exposed 3′-end for displacing the downstream DNA strand (secondary target, abbreviated ST). Subsequently, the ST strand could open the capture DNA (cDNA) immobilized sensing surface for baring the toehold of cDNA to capture ABEI-labeled S hairpin DNA (ABEI-S). Notably, the laccase was anchored Au nanoparticles-wrapped TiO_2 nanoparticles (TiO_2@Au) modified electrode surface, which efficiently promoted the reduction of dissolved O_2 to generate the strong oxidizing intermediate superoxide radical ($O_2^{\bullet-}$) for remarkably enhancing ECL signal of ABEI. As a result, the sensing platform exhibited relatively wide detection range of 100 aM to 100 pM with a detection limit of 80.8 aM for the determination of miR-21. It manifested that the proposed ternary system with excellent biocompatibility and dramatically enhanced ECL emission has promising applications in the realm of biological analysis.

Experimental

Preparation of TiO_2@Au nanocomposite

The TiO_2 nanoparticles was synthesized based on reported literature [11] with some modifications, and then the Au nanoparticles-wrapped TiO_2 nanoparticles (TiO_2@Au) was synthesized as follows. Specifically, 10 mg TiO_2 powder was ultrasonic dispersed in 1 mL deionized water to obtain milk white homogeneous solution. Next, 300 μL 1% polyethyleneimine (PEI) was added into the solution for stirring 1 h at room temperature. Five hundred microliters of 1 mM $HAuCl_4$ was successively treated with PEI-functionalized TiO_2 nanoparticles under vigorous stirring. Two minutes later,

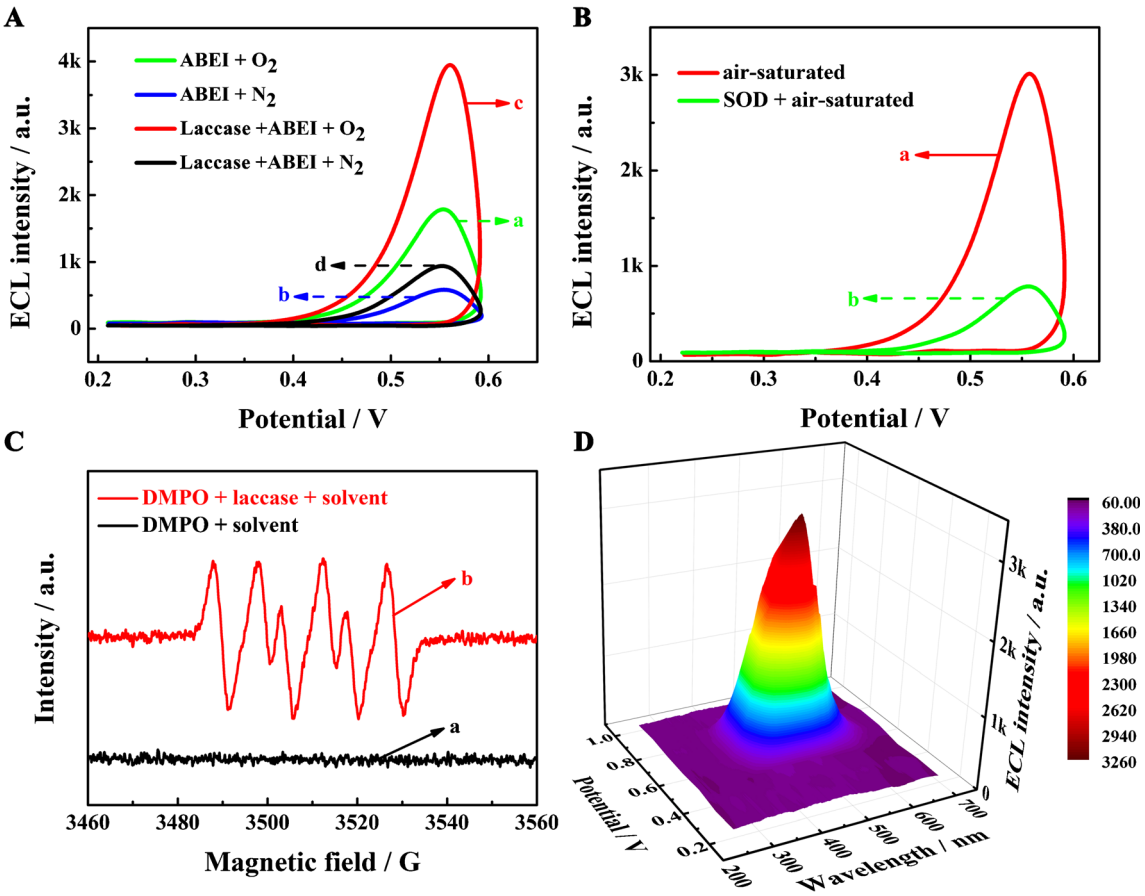

Fig. 1 (**A**) The ECL response of different electrodes in diverse conditions: the bare GCE in air-saturated PBS (curve a), N_2-saturated PBS (curve b), 2 mg/mL laccase plus air-saturated PBS (curve c), and 2 mg/mL laccase plus N_2-saturated PBS (curve d). (**B**) The ECL potential profiles of bare GCE in 2 mg/mL laccase plus air-saturated PBS (curve a), 2 mg/mL laccase, and 10 U·mL^{-1} SOD plus air-saturated PBS (curve b). (**C**) The EPR spectrum of PBS (pH 7.4) containing 100 mM DMPO (curve a), 100 mM DMPO +1 mM laccase (curve b). (**D**) The 3D surface image of the proposed ECL ternary system. The above experiments were measured in the detection solution containing 3.75 mM ABEI

100 μL of 1 mM $NaBH_4$ was dropwise introduced into the mixed solution and then constantly stirred at room temperature for 1 h. After the process of centrifugation and purification, the TiO_2@Au precipitation was dissolved in water to generate 5 mg/mL stock solution.

The preparation of secondary target

The secondary target (ST) was prepared by the strand displacement amplification. Firstly, the annealed hairpin template (1 μM) and targets of various concentrations were mixed by equal volume, and then incubated at 37 °C for 1 h to generate the template-miR-21 complex. Afterwards, 500 μM deoxyribonucleoside triphosphates (dNTPs), 100 U/mL Nt.BsmAI, and 100 U/mL phi 29 DNA polymerase were added into above mixture and incubated for at 37 °C to generate masses of ST. After 2 h, the mixed solution was heated to 65 °C for 10 min to inactivate the Nt.BsmAI, and stored at 4 °C for further use.

The synthesis of S-ABEI complex

Primarily, the carboxyl hairpin DNA (S) was annealed in 5 min at 95 °C to form the hairpin structure. Then 50 μL 2 μM S, 5 μL 400 mM 1-(3-dimethylaminopropyl) -3-ethylcarbodiimide hydrochloride (EDC), and 5 μL 100 mM N-hydroxysuccinimide (NHS) were mixed and incubated for 20 min at room temperature to activate the carboxyl group. Subsequently, 5 μL 25 mM N-(aminobutyl)-N-(ethylisoluminol) (ABEI) was added into the mixture for 2 h at room temperature to form amido bond. Eventually, the obtained ABEI-labeled S hairpin DNA (ABEI-S) was stored at 4 °C for further use. In addition, the UV-Vis spectrum was employed to verify the generation of ABEI-S complex and the characterization results presented in Fig. S1.

The assembly process and detection procedure of biosensor

The assembly process of the ECL biosensor was shown in Scheme 1B. Above all, the bare glassy carbon electrode

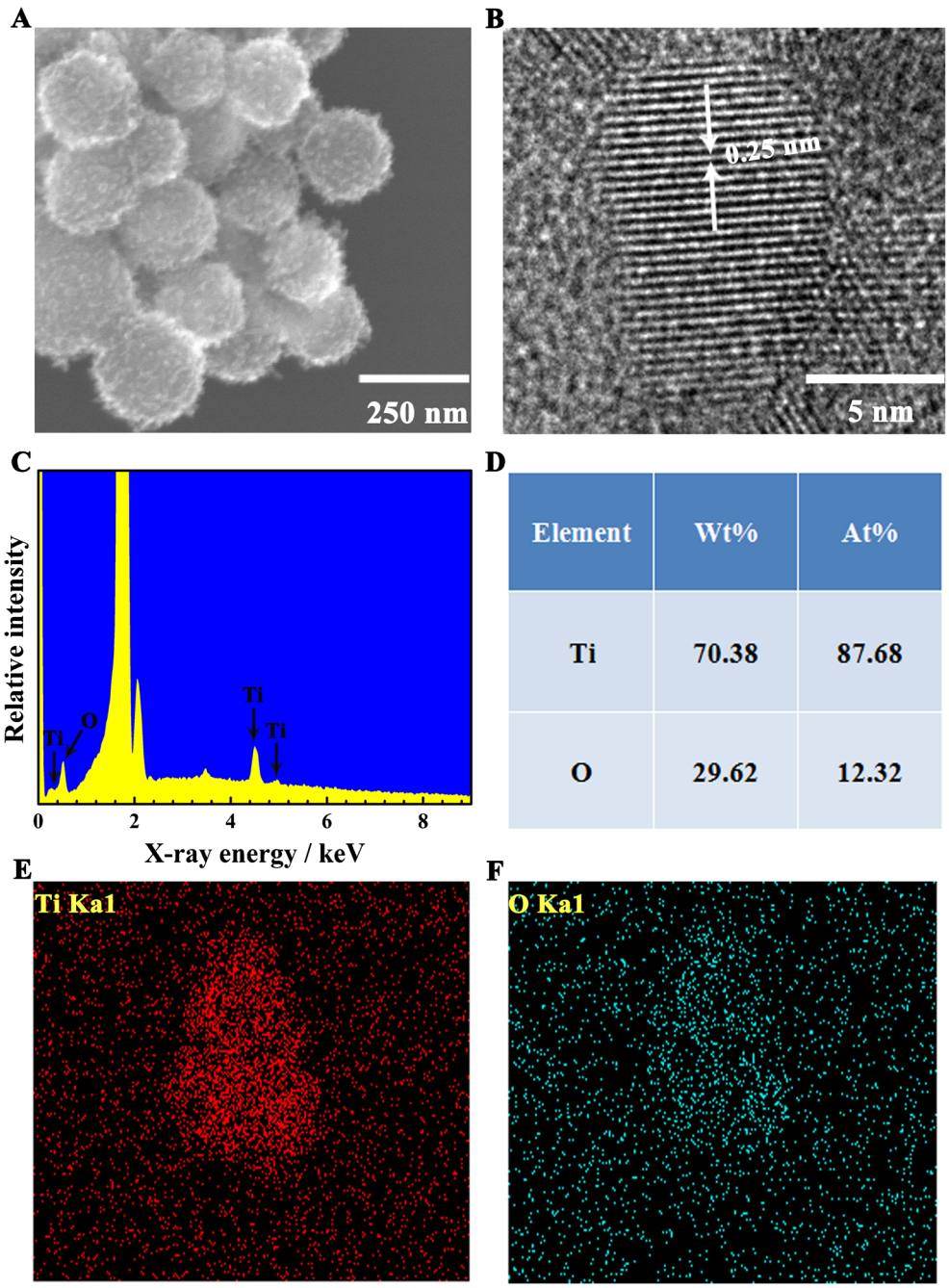

Fig. 2 (**A**) SEM and (**B**) TEM characterization analysis of the TiO_2. (**C**) The total EDS spectrum and (**D**) the element distribution of the TiO_2. The element image of Ti (**E**) and O (**F**)

(GCE) was polished with 0.3 and 0.05 μm aluminum slurry and then alternately ultrasonic washed with deionized water and ethanol. Afterwards, 5 μL prepared TiO_2@Au was fixed on the clear electrode surface and dried at room temperature via well film-forming property of TiO_2. Following that, 10 μL 1 μM annealed the capture DNA (cDNA) was modified on the electrode for 12 h at 4 °C to obtain Au-S bond. The modified electrode was blocked with 10 μL 2 mg/mL laccase at 25 °C for 40 min. Subsequently, the ST related to different concentrations of the target was dropped on the sensing surface for 1 h at 25 °C to open the hairpin cDNA. Ultimately, 10 μL ABEI-S as signal probe was fixed on the electrode at 25 °C for 2 h through the base pairing of S and the toehold of cDNA. Notably, after each step of incubation, the electrodes were washed by PBS solution to remove unreacted reagent. Simultaneously, the cyclic voltammetry (CV) and ECL were performed to explore the fabrication of the biosensor (Fig. S3). Finally, the proposed sensing platform was investigated in the 3 mL of air-saturated 0.1 M PBS (pH 8.0) at the scan voltage from 0.2 to 0.6 V with the scan rate of 300 mV/s.

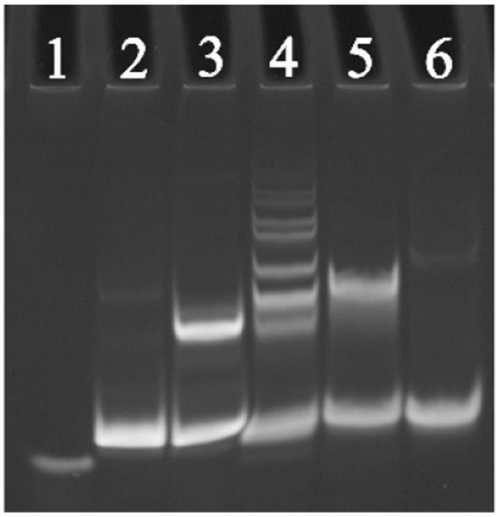

Fig. 3 The PAGE images of different samples: lane 1: miR-21; lane 2: template; lane 3: the mixture of miR-21 and template; lane 4: the mixture of miR-21, template, dNTPs, and phi 29 DNA polymerase; lane 5: the mixture of miR-21, template, dNTPs, Nt.BsmAI, and phi 29 DNA polymerase; lane 6: the mixture of template, dNTPs, Nt.BsmAI, and phi 29 DNA polymerase

Results and discussion

The ECL possible mechanism of ABEI/dissolved O_2 system in the acceleration of laccase

ECL responses of different electrodes were measured under the diverse conditions to investigate the mechanism of the proposed system. As shown in Fig. 1A, a weak ECL emission at 585 a.u. was observed from the bare GCE in N_2-saturated PBS containing 3.75 mM ABEI (curve b), but the ECL response increased to 1800 a.u. in air-saturated PBS (curve a), the saturated oxygen in detection solution significantly promoted the ECL signal of ABEI, so that it was defined as the coreactant. After the laccase was added into the binary system, the ECL intensity zoomed to around 4000 a.u. (curve c). Nevertheless, the bare GCE in 3.75 mM ABEI and 2 mg/mL laccase solution after purging with N_2 for 30 min just possessed a weak ECL response at 1000 a.u. (curve d). Those results demonstrated that ABEI could reveal excellent ECL performance in the combination of the dissolved O_2 as the coreactant and the laccase as the coreaction accelerator.

More interestingly, when superoxide dismutase (SOD) was introduced into the ternary system to consume $O_2^{\bullet-}$, the bare GCE in air-saturated PBS (Fig. 1B, curve b) showed an exceedingly feeble ECL response comparing with that of ECL ternary system in air-saturated (curve a). This reflected that the $O_2^{\bullet-}$ acted as an essential intermediate in the ECL system. In addition, the electron spin resonance (EPR) pattern was performed to visually verify the coreaction acceleration of laccase in air-saturated PBS. As displayed in Fig. 1C, an obvious sextet characteristic peak of 5,5-dimethyl-1-pyrroline N-oxide (DMPO)-$O_2^{\bullet-}$ could be seen from PBS containing 20% ethanol solution and 2 mg/mL laccase (curve b) in comparison with the absence of laccase (curve a), which was consistent with the reported work [12]. According to the results, we drew a conclusion that the laccase could efficiently biocatalyze dissolved O_2 to generated more $O_2^{\bullet-}$, facilitating the ECL response of the ternary system. Moreover, the spectrum analysis of bare GCE was conducted in 2 mL PBS containing 3.75 mM ABEI and 2 mg/mL laccase. The maximum ECL emission was located at 472 nm (Fig. 1D), which was same as the value of ABEI in the published report [13]. The above results further stated that the bioenzyme could be an excellent candidate to act as biocompatible coreaction accelerator for strong enhancing the ECL response of binary ECL system.

Table 1 Comparison of our methods with others for miRNA determination

Methods	Detection limit	Dynamic range	Ref
Electrochemistry	0.34 fM	1 fM-1 nM	[14]
Photoelectrochemistry	2.4 aM	100 aM-1 nM	[15]
Fluorescence	2.27 fM	50 fM-10 nM	[16]
THz spectroscopy	14.54 aM	1 fM-10 pM	[17]
ECL	60 fM	500 fM-1 nM	[18]
ECL	80.8 aM	100 aM-100 pM	This work

Characterization analysis of the TiO_2 NPs

Furthermore, scanning electron microscopy (SEM) and transmission electron microscopy (TEM) images revealed that the synthesized TiO_2 nanoparticles exhibited dispersive and uniform spherical particles with about 200 nm in diameter. A closer observation by magnified HR-TEM investigation (Fig. 2B) presented the TiO_2 with well-defined 2D lattice fringes of 0.25 nm, which was close to the (101) lattice spacing of face-centered cubic (fcc) unit, suggesting the single-crystal structure of the prepared TiO_2. Subsequently, the energy dispersion spectrum (EDS) of TiO_2 was explored to investigate its element distribution. It can be seen from Fig. 2C, the TiO_2 was composed by the element of Ti and O at the percentage composition ratio of approximately 1.6:1 (Fig. 2D), while the same results could obtain through scanning TEM coupled with energy dispersive X-ray (STEM-EDX) spectroscopy (Fig. 2E and F). The above results suggested that the TiO_2 was successfully prepared.

The characterization of strand displacement amplification

The native polyacrylamide gel electrophoresis (PAGE) was performed to confirm the practicability of the strand displacement amplification (SDA) reaction. As shown in Fig. 3, two single bands could be seen in lane 1 and lane 2, which

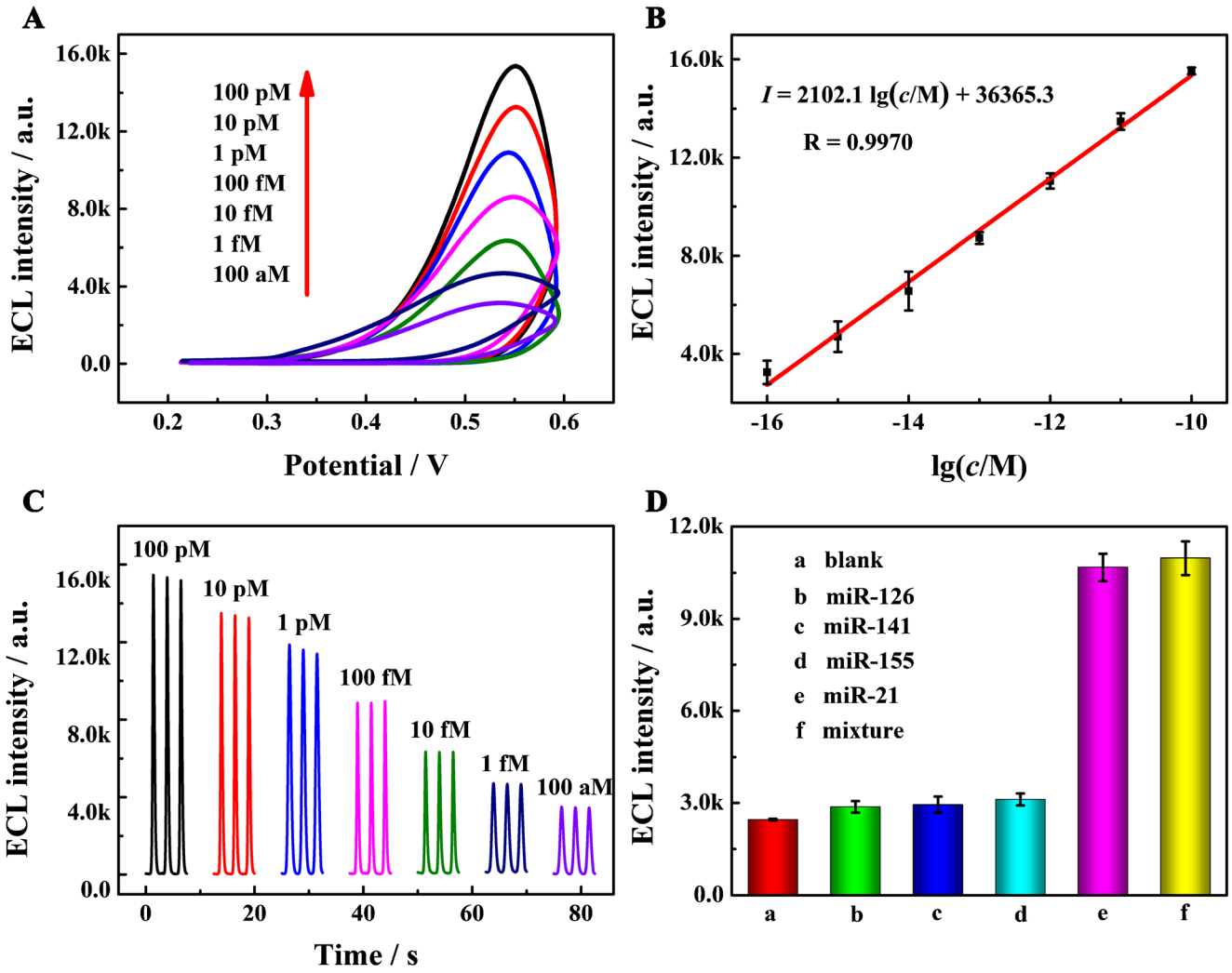

Fig. 4 (**A**) The ECL responses of different concentration of miR-21. (**B**) The linear relationship between ECL intensity and the logarithm of miR-21 concentration. (**C**) Stability and (**D**) selectivity performances of the biosensor for detecting miR-21

represented the target miR-21 and template, respectively. When the miR-21 hybridized with template at 37 °C for 60 min, the band in lane 3 displayed a slow mobility with higher molecular weight. Simultaneously, the dNTPs and phi 29 DNA polymerase were added into the hybridization of target and template, many bands could be seen in lane 4, one of them was the unreacted template which had the same position with the pure template, and the others represented the amplification products of miR-21 and the template in the presence of phi 29 DNA polymerase and dNTPs. Successively, once dNTPs, Nt.BsmAI, and phi 29 DNA polymerase were added into the hybridization product, three distinct bands could be seen in lane 5. The highest band was the amplification products of miR-21 and template, and the middle band might be the unreacted template, while the lowest band ascribed to the secondary target (ST) owing to the presence of Nt.BsmAI. In addition, the mixture of template, dNTPs, Nt.BsmAI, and phi 29 DNA polymerase without miR-21were analyzed. Two bands could be seen in lane 6, which severally stood for the amplification products of template and unreacted template. The above results proved that the proposed SDA reaction was reasonable and practicable.

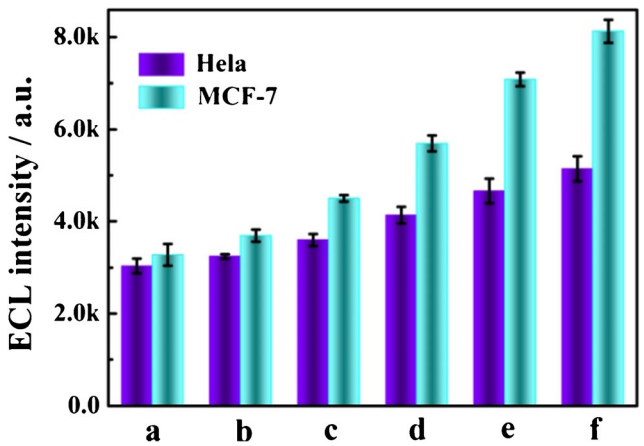

Fig. 5 ECL intensity of the various lysates concentration from MCF-7 cancer cells and HeLa cancer cells: (a) 10 cells, (b) 10^2 cells, (c) 10^3 cells, (d) 10^4 cells, (e) 10^5 cells, (f) 10^6 cells

The analytical performance of the sensing platform

To examine the potential application of the ECL biosensor for miR-21 determination, a variety of concentrations of miR-21 were investigated under the optimal conditions (the optimization condition was displayed in Fig. S2). In Fig. 4A, the ECL response enhanced with the increasing of miR-21 concentration. Simultaneously, the linear relationships for the ECL intensity (I) to the logarithmic value of miR-21 concentration ($\lg c$) in the range of 100 aM to 100 pM were expressed as $I = 2102.1 \lg(c/\mathrm{M}) + 36{,}365.3$, with a correlation coefficient of 0.9970 (Fig. 4B). The limit of detection (LOD) was calculated to be 80.8 aM ($S/N = 3$), compared with other reported methods for miRNA determination to attest a satisfactory sensitivity of the proposed biosensor (Table 1).

Furthermore, the stability and selectivity of the biosensor were vital factory to assess the availability. As shown in Fig. 4C, the ECL intensity at each concentration could be stable for three cycles, proving that the proposed biosensor possessed benign stability. Besides, the selectivity of ECL biosensor was investigated from the response of electrodes which was fabricated by 100 pM miR-155, 100 pM miR-141, and 100 pM miR-126 replacing the 1 pM miR-21, respectively. As can be seen from Fig. 4D, the ECL intensity of blank was almost identical to miR-155, miR-141, and miR-126, while the ECL response in the presence of 1 pM target presented high-intense intensity which was close to the mixture consist of 100 pM miR-155, 100 pM miR-141, and 100 pM miR-126, and 1 pM miR-21. Those results suggested that the developed biosensor had remarkable specificity. Moreover, the relative standard deviation (RSD) of intra-assays and inter-assays were evaluated as respectively 4.80% and 4.41% (the detailed calculation process shown in Fig. S4), indicating great reproducibility of the proposed biosensor.

The feasibility analysis of the proposed biosensor

The applicability of the sensing platform in actual samples was investigated by detecting miR-21 in human cervical cancer cell line (HeLa) and human breast cancer cell line (MCF-7). As displayed in Fig. 5, the ECL intensity distinctly increased with the increasing of the MCF-7 cell numbers (a-f), while the slightly changed with the increasing of the Hela cell numbers (a-f). Those results indicated that the miR-21 overexpressed in MCF-7 and under-expressed in Hela, identifying with previously reported research [19, 20]. Thus, the proposed biosensor could be applied to actual detection.

Conclusions

In conclusion, the laccase was first defined biocoreaction accelerator to biocatalyze the reduction of dissolved O_2 for significantly boosting the ECL efficiency of ABEI; thus, the ternary system possessed strong enhanced ECL performance. Whereafter, improved SDA was realized by replacing traditional single strand DNA to the hairpin DNA as template for high efficiency triggering the immobilization of more signal probes, achieving the ultrasensitive detection of miR-21. Moreover, the developed sensing platform had good performance of monitoring miRNA from cancer cells. From the above, this sensing platform possesses excellent prospects in biological analysis and clinical diagnosis.

Supplementary Information The online version contains supplementary material available at https://doi.org/10.1007/s00604-021-04854-6.

Funding This work was financially supported by the NNSF of China (21974108, and 21775124), and Postdoctoral Science Foundation of China (2019 M663418).

Declarations

Conflict of interest The authors declare that they have no competing interests.

References

1. Maar RR, Zhang RZ, Stephens DG, Ding ZF, Gilroy JB (2019) Near-infrared photoluminescence and electrochemiluminescence from a remarkably simple boron difluoride formazanate dye. Angew Chem Int Ed 58:1052–1056
2. Zhang P, Jiang J, Yuan R, Zhuo Y, Chai Y (2018) Highly ordered and field-free 3D DNA nanostructure: the next generation of DNA nanomachine for rapid single-step sensing. J Am Chem Soc 140: 9361–9364
3. Zanut A, Palomba F, Scota M, Rebeccani S, Marcaccio M, Genovese D, Rampazzo E, Valenti G, Paolucci F, Prodi L (2020) Chameleon metals: autonomous nano-texturing and composition inversion on liquid metals surfaces. Angew Chem Int Ed 59:1
4. Ying Z, Chen S, Luo X, Chai Y, Yuan R (2018) Ternary electrochemiluminescence nanostructure of Au nanoclusters as a highly efficient signal label for ultrasensitive detection of cancer biomarkers. Anal Chem 90:10024
5. Tang TT, Yang F, Wang L, Zhao CX, Nie F, Yang GP (2020) A sandwich electrochemiluminescent assay for determination of concanavalin A with triple signal amplification based on MoS_2NF@MWCNTs modified electrode and Zn-MOF encapsulated luminol. Microchim Acta 187:523
6. Gu W, Wang H, Jiao L, Wu Y, Chen Y, Hu L, Gong J, Du D, Zhu C (2020) Single-atom iron boosts electrochemiluminescence. Angew Chem Int Ed 59:3534–3538
7. Xing HH, Peng C, Xue Y, Fan YC, Li J, Wang EK (2020) In situ formed catalytic interface for boosting chemiluminescence. Anal Chem 92:10108–10113
8. Liu JL, Tang ZL, Zhuo Y, Chai YQ, Yuan R (2017) Ternary electrochemiluminescence system based on rubrene microrods as luminophore and Pt nanomaterials as coreaction accelerator for ultrasensitive detection of microRNA from cancer cells. Anal Chem 89(17):9108–9115
9. Zhang R, Chen AY, Yu YQ, Chai YQ, Zhuo Y, Yuan R (2018) Electrochemiluminescent carbon dot-based determination of

microRNA-21 by using a hemin/G-wire supramolecular nanostructure as co-reaction accelerator. Microchim Acta 185:432

10. Wu FF, Zhou Y, Zhang H, Yuan R, Chai YQ (2018) Electrochemiluminescence peptide-based biosensor with hetero-nanostructures as coreaction accelerator for the ultrasensitive determination of tryptase. Anal Chem 90(3):2263–2270
11. Pan J, Wang X, Huang Q, Shen C, Koh Z, Wang Q, Engel A, Bahnemann DW (2014) Large-scale synthesis of urchin-like mesoporous TiO_2 hollow spheres by targeted etching and their photoelectrochemical properties. Adv Funct Mater 24:95–104
12. Roberts JG, Voinov AM, Schmidt AC, Smirnova TI, Sombers LA (2016) The hydroxyl radical is a critical intermediate in the voltammetric detection of hydrogen peroxide. J Am Chem Soc 138:2516–2519
13. Fang DD, Zeng BS, Zhang SP, Dai H, Lin YY (2020) A self-enhanced electrochemiluminescent ratiometric zearalenone immunoassay based on the use of helical carbon nanotubes. Microchim Acta 187:303
14. Bruch R, Baaske J, Chatelle C, Meirich M, Madlener S, Weber W, Dincer C, Urban G (2019) CRISPR/Cas13a-powered electrochemical microfluidic biosensor for nucleic acid amplification-free miRNA diagnostics. Adv Mater 31:1905311
15. Liu L, Yao Y, Ma KJ, Shangguan CJ, Jiao SL, Zhu SY, Xu XX (2021) Ultrasensitive photoelectrochemical detection of cancer-related miRNA-141 by carrier recombination inhibition in hierarchical Ti_3C_2@ReS_2. Sensors Actuators B Chem 331:129470
16. Xian L, Ge H, Xu F, Xu N, Fan J, Shao K, Peng X (2019) Intracellular microRNA imaging using telomerase-catalyzed FRET ratioflares with signal amplification. Chem Sci 10:7111–7118
17. Yang K, Li JN, de la Chapelle ML, Huang GR, Wang YX, Zhang JB, Xu DG, Yao JQ, Yang X, Fu WL (2021) A terahertz metamaterial biosensor for sensitive detection of microRNAs based on gold-nanoparticles and strand displacement amplification. Biosens Bioelectron 175:112874
18. Ye J, Liu G, Yan M, Zhu Q, Zhu L, Huang J, Yang X (2019) Highly luminescent and self-enhanced electrochemiluminescence of tris(bipyridine) ruthenium(II) nanohybrid and its sensing application for label-free detection of microRNA. Anal Chem 91:13237–13243
19. Xue C, Zhang S, Ouyang C, Chang D, Salena B, Li Y, Wu Z (2018) Target-induced catalytic assembly of Y-shaped DNA and its application for in situ imaging of microRNAs. Angew Chem Int Ed 57:9739–9743
20. Yan N, Wang XJ, Lin L, Song TJ, Sun PJ, Tian HY, Liang HJ, Chen XS (2018) Gold nanorods electrostatically binding nucleic acid probe for in vivo microRNA amplified detection and photoacoustic imaging-guided photothermal therapy. Adv Funct Mater 28:1800490